

Large diamagnetic persistent currents

Sheelan Sengupta Chowdhury¹, P. Singha Deo¹, Ashim Kumar Roy² and M. Manninen³

¹*Unit for Nanoscience and Technology,*

S. N. Bose National Centre for Basic Sciences,

Sector-III, Block-JD, Salt Lake, Kolkata-700098, India

²*Physics and applied mathematics unit, Indian Statistical Institute,*

203, B. T. Road, Kolkata-700108, India

³*Nanoscience center, Department of Physics,*

University of Jyväskylä, P.O. Box-35, 40014, Jyväskylä, Finland.

Abstract

In multichannel rings, evanescent modes will always co-exist with propagating modes. The evanescent modes can carry a very large diamagnetic persistent current that can oscillate with energy and are very sensitive to impurity scattering. This provides a natural explanation for the large diamagnetic persistent currents observed in experiments.

PACS numbers:

Büttiker, Imry and Landauer first suggested the possibility of observing persistent current in normal metal or semiconducting rings threaded by an Aharonov-Bohm flux¹. This current is an equilibrium property of the ring, given by the flux derivative of the total energy of the ring. Since then several experiments have been done that confirm the existence of persistent current in such rings^{2,3,4,5,6,7,8,9} through magnetization measurements. However, the nature of these currents are quite different from what is expected theoretically^{10,11}. While earlier experiments^{2,3,4,5,6,7,8} had some ambiguity, recent experiments made on an ensemble of 10^5 rings have made very careful measurements of the sign (positive implies diamagnetic and negative implies paramagnetic) and periodicity of the persistent current⁹. If an ensemble of rings is taken, one can calculate an ensemble average over the number of electrons in different rings or over disorder, or over both¹⁰. In such cases one finds that the ensemble average has $\phi_0/2$ (or $hc/2e$) periodicity and the low field persistent current is paramagnetic in nature. One can also take a fixed chemical potential and average over disorder. Here again one can calculate to find paramagnetic persistent current with $\phi_0/2$ periodicity¹¹. Whereas, the experiment⁹ shows a persistent current, that has $\phi_0/2$ periodicity but diamagnetic in nature at low fields and also of a large magnitude (10 to 100 times larger than that theoretically estimated in the above mentioned models of ensemble averaging).

Any quantity that is very sensitive to disorder will average to zero. But the second harmonic do not obey this rule and gives nonzero value. This is essentially because the second harmonic consists of time reversed trajectories and disorder configuration does not change the observed quantity randomly. This is very robust and manifests in a variety of phenomena briefly described below. Weak localization in disordered metallic or semi-conducting samples occur because of this. Forward scattering probability beyond a certain length turns out to be negligibly small while the back scattering arising due to time reversed trajectories always interfere constructively, irrespective of disorder configuration. As a consequence the Aronov-Altshuler-Spivak weak localization correction to conductance has $\phi_0/2$ periodicity¹². Also the response of a long cylinder to an applied magnetic field turns out to have $\phi_0/2$ periodicity¹³. $\phi_0/2$ periodicity of ensemble averaged persistent current is due to the same reason that the first harmonic averages to zero while the second does not.

The first attempt to explain the discrepancy in sign and magnitude is based on repulsive interactions between electrons^{11,14}. This did not turn out to be the correct mechanism because this yields a paramagnetic response at low fields whereas recent experiment has conclusively shown that the observed response is diamagnetic. For a recent analysis of the effect of disorder and interactions, we refer [15]. A more recent attempt to explain the experimental discrepancy is based on additional currents that may be generated in rings due to the rectification of a high frequency non-equilibrium noise¹⁶. This mechanism can give a diamagnetic current in absence of spin orbit coupling and a paramagnetic response in presence of spin orbit coupling. Recent experiment⁹ has also ruled out this explanation as paramagnetic response could not be observed in presence of strong spin orbit coupling. The origin of a high frequency non-equilibrium noise also seems to be unclear.

All experiments have been done at finite temperatures. There are thermal effects wherein an electron can get energy from some collision and get excited to higher states. Such inelastic processes will not destroy the persistent currents. Persistent currents are actually observed in networks, where total length is much greater than the inelastic mean free path¹⁷. When a mechanism for excitation is present then evanescent modes can be excited. It has been shown that in a one dimensional (1D) ring, evanescent modes can carry a diamagnetic persistent current. It has a very small magnitude compared to persistent current in propagating modes and cannot exhibit $\phi_0/2$ periodicity as it is not sensitive to disorder. Rings used in the experiments have a finite thickness and are referred to as quasi-one dimensional (Q1D) rings. In this work we show that in Q1D, evanescent modes can carry very large diamagnetic persistent current that are comparable to that of propagating modes and are as sensitive to disorder as that due to the propagating modes. So this mechanism is a natural explanation for the observed diamagnetic persistent current.

In this work we use a simple technique to excite evanescent modes. We consider the ring to be coupled to an infinite wire as schematically shown in Figure 1. This basically constitutes an open system and it is known that it can simulate the effects of inelastic collisions and thermal effects¹⁹. We shall see in our mathematical analysis how evanescent modes are excited in this

system very naturally. We consider two modes of propagation as the results can be generalized to any number of modes. There is a δ -potential impurity present in the ring at any arbitrary position X [Fig 1]. We apply Aharonov-Bohm flux ϕ through the ring, perpendicular to the plane of the paper. The Schrödinger equation for a Q1D wire in presence of a δ -potential at $x = 0, y = y_i$ is

$$\left[-\frac{\hbar^2}{2m}\left(\frac{\partial^2}{\partial x^2} + \frac{\partial^2}{\partial y^2}\right) + V_c(y) + \gamma\delta(y - y_i)\delta(x)\right]\Psi(x, y) = E\Psi(x, y) \quad (1)$$

Here V_c is the confinement potential making up the quantum wires in Figure 1. Solutions to Schrödinger equation in a ring geometry can be obtained by applying periodic boundary conditions to Eqn. 1. The magnetic field just appears as a phase of $\Psi(x, y)$ that will be accounted for while applying boundary conditions. Away from the scattering regions Eqn. 1 can be separated as

$$-\frac{\hbar^2}{2m}\frac{d^2\psi(x)}{dx^2} = \frac{\hbar^2 k^2}{2m}\psi(x) \quad (2)$$

and

$$\left[-\frac{\hbar^2}{2m}\frac{d^2}{dy^2} + V_c(y)\right]\chi_n(y) = E_n\chi_n(y) \quad (3)$$

Here we take V_c to be a square well potential of width W that gives $\chi_n(y) = \sin\left[\frac{n\pi}{W}\left(y + \frac{W}{2}\right)\right]$. In the first mode, $k_1 = \sqrt{\frac{2mE}{\hbar^2} - \frac{\pi^2}{W^2}}$ and in the second mode $k_2 = \sqrt{\frac{2mE}{\hbar^2} - \frac{4\pi^2}{W^2}}$ are the propagating wave-vectors. m is the electron mass, E is the electron energy and W is the width of the quantum wire. When electrons are incident along region I (in Fig 1) in the first mode the scattering problem can be solved exactly. The solution to Eqn. 2 in region I becomes

$$\psi_I = \frac{1}{\sqrt{k_1}}e^{ik_1x} + \frac{r'_{11}}{\sqrt{k_1}}e^{-ik_1x} + \frac{r'_{12}}{\sqrt{k_2}}e^{-ik_2x} \quad (4)$$

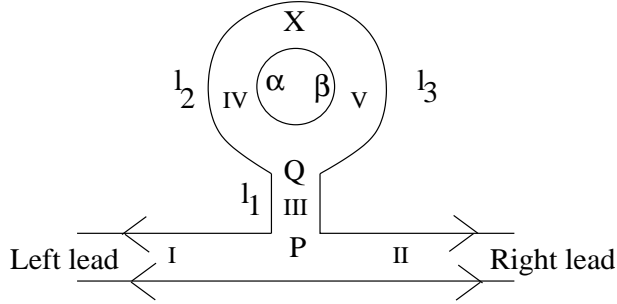


FIG. 1: A ring connected with an infinite wire. A δ -potential impurity is at position X .

Similarly, in region II , III , IV and V we get

$$\psi_{II} = \frac{g'_{11}}{\sqrt{k_1}} e^{ik_1 x} + \frac{g'_{12}}{\sqrt{k_2}} e^{ik_2 x} \quad (5)$$

$$\psi_{III} = \frac{Ae^{ik_1 y}}{\sqrt{k_1}} + \frac{Be^{-ik_1 y}}{\sqrt{k_1}} + \frac{Ce^{ik_2 y}}{\sqrt{k_2}} + \frac{De^{-ik_2 y}}{\sqrt{k_2}} \quad (6)$$

$$\psi_{IV} = \frac{Ee^{ik_1 z}}{\sqrt{k_1}} + \frac{Fe^{-ik_1 z}}{\sqrt{k_1}} + \frac{Ge^{ik_2 z}}{\sqrt{k_2}} + \frac{He^{-ik_2 z}}{\sqrt{k_2}} \quad (7)$$

$$\psi_V = \frac{Je^{ik_1(z-l_2)}}{\sqrt{k_1}} + \frac{Ke^{-ik_1(z-l_2)}}{\sqrt{k_1}} + \frac{Le^{ik_2(z-l_2)}}{\sqrt{k_2}} + \frac{Me^{-ik_2(z-l_2)}}{\sqrt{k_2}} \quad (8)$$

The lead is along x direction and region III is along y direction. z is used to denote coordinate inside the ring, the geometry of the ring being taken care of by applying periodic boundary conditions to z . r'_{11} , r'_{12} , g'_{11} and g'_{12} are the scattering matrix elements and A , B , C , D , E , F , G , H , J , K , L , M are to be determined by mode matching.

Note that at P and Q we have a three legged junction that is schematically shown in Fig.

2. So far a popularly used scattering matrix for a three-legged junction is²⁰

$$S_U = \begin{pmatrix} -(a_s + b_s) & 0 & \sqrt{\epsilon} & 0 & \sqrt{\epsilon} & 0 \\ 0 & -(a_s + b_s) & 0 & \sqrt{\epsilon} & 0 & \sqrt{\epsilon} \\ \sqrt{\epsilon} & 0 & a_s & 0 & b_s & 0 \\ 0 & \sqrt{\epsilon} & 0 & a_s & 0 & b_s \\ \sqrt{\epsilon} & 0 & b_s & 0 & a_s & 0 \\ 0 & \sqrt{\epsilon} & 0 & b_s & 0 & a_s \end{pmatrix} \quad (9)$$

with $a_s = \frac{1}{2}(\sqrt{1-2\epsilon} - 1)$, $b_s = \frac{1}{2}(\sqrt{1-2\epsilon} + 1)$ and $0 < \epsilon < 0.5$. Such junction S -matrix does not include channel mixing and can not account for any contribution from evanescent modes.

In this work we propose a three-legged junction scattering matrix S_J for a two channel quantum wire that can be easily generalized to any number of channels. It is given by

$$S_J = \begin{pmatrix} r_{11} & r_{12} & g_{11} & g_{12} & f_{11} & f_{12} \\ r_{21} & r_{22} & g_{21} & g_{22} & f_{21} & f_{22} \\ g_{11} & g_{12} & r_{11} & r_{12} & f_{11} & f_{12} \\ g_{21} & g_{22} & r_{21} & r_{22} & f_{21} & f_{22} \\ f_{11} & f_{12} & f_{11} & f_{12} & r_{11} & r_{12} \\ f_{21} & f_{22} & f_{21} & f_{22} & r_{21} & r_{22} \end{pmatrix} \quad (10)$$

where

$$\begin{aligned} r_{11} &= -\frac{3k_2 + k_1}{3k_1 + 3k_2} \\ g_{11} = f_{11} &= \frac{2k_1}{3k_1 + 3k_2} \\ r_{12} = g_{12} = f_{12} &= \sqrt{\frac{k_2}{k_1}} \frac{2k_1}{3k_1 + 3k_2} \\ r_{22} &= -\frac{3k_1 + k_2}{3k_1 + 3k_2} \\ g_{22} = f_{22} &= \frac{2k_2}{3k_1 + 3k_2} \\ r_{21} = g_{21} = f_{21} &= \sqrt{\frac{k_1}{k_2}} \frac{2k_2}{3k_1 + 3k_2} \end{aligned} \quad (11)$$

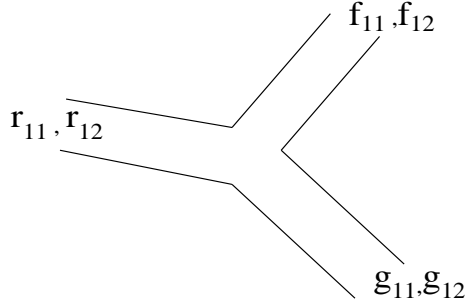


FIG. 2: A 3-leg junction.

Mode matching at the junction P [Fig. 1] gives

$$\begin{pmatrix} r'_{11} \\ r'_{12} \\ g'_{11} \\ g'_{12} \\ A \\ C \end{pmatrix} = S_J \begin{pmatrix} 1 \\ 0 \\ 0 \\ 0 \\ B \\ D \end{pmatrix} \quad (12)$$

Similarly, mode matching at the junction Q [Fig. 1] gives

$$\begin{pmatrix} B e^{-ik_1 l_1} \\ D e^{-ik_2 l_1} \\ E \\ G \\ K e^{-ik_1 l_3} \\ M e^{-ik_2 l_3} \end{pmatrix} = S_J \begin{pmatrix} A e^{ik_1 l_1} \\ C e^{ik_2 l_1} \\ F e^{-i\alpha} \\ H e^{-i\alpha} \\ J e^{i(k_1 l_3 + \beta)} \\ L e^{i(k_2 l_3 + \beta)} \end{pmatrix} \quad (13)$$

Here l_1 , l_2 and l_3 are shown in Fig. 1. $\alpha + \beta = 2\pi\phi/\phi_0$, ϕ being the magnetic flux and $\phi_0 = hc/e$ is the flux quantum. Eqn. 13 automatically applies periodic boundary conditions to

wave function in the ring. Mode matching at the impurity site X [Fig. 1] gives

$$\begin{pmatrix} F e^{-ik_1 l_2} \\ H e^{-ik_2 l_2} \\ J \\ L \end{pmatrix} = \begin{pmatrix} \tilde{r}_{11} & \tilde{r}_{12} & \tilde{t}_{11} & \tilde{t}_{12} \\ \tilde{r}_{21} & \tilde{r}_{22} & \tilde{t}_{21} & \tilde{t}_{22} \\ \tilde{t}_{11} & \tilde{t}_{12} & \tilde{r}_{11} & \tilde{r}_{12} \\ \tilde{t}_{21} & \tilde{t}_{22} & \tilde{r}_{21} & \tilde{r}_{22} \end{pmatrix} \times \begin{pmatrix} E e^{i(k_1 l_2 + \alpha)} \\ G e^{i(k_2 l_2 + \alpha)} \\ K e^{-i\beta} \\ M e^{-i\beta} \end{pmatrix} \quad (14)$$

where ²¹,

$$\tilde{r}_{pp'} = \frac{-i \frac{\Gamma_{pp'}}{2\sqrt{k_p k_{p'}}}}{1 + \sum_e \frac{\Gamma_{ee}}{2\kappa_e} + i \sum_p \frac{\Gamma_{pp}}{2k_p}} \quad (15)$$

\sum_e represents sum over all the evanescent modes and \sum_p represents sum over all the propagating modes. p or p' can take values 1 and 2 as there are two propagating modes. $\kappa_e = \sqrt{\frac{e^2 \pi^2}{W^2} - \frac{2mE}{\hbar^2}}$, where $e = 3, 4, \dots$. The inter-mode (i.e. $p \neq p'$) transmission amplitudes are $\tilde{t}_{pp'} = \tilde{r}_{pp'}$ and intra-mode transmission amplitudes are $\tilde{t}_{pp} = 1 + \tilde{r}_{pp}$. $\Gamma_{pp'}$ is given as

$$\Gamma_{pp'} = \frac{2m\gamma}{\hbar^2} \sin\left[\frac{p\pi(q + W/2)}{W}\right] \sin\left[\frac{p'\pi(q + W/2)}{W}\right] \quad (16)$$

where q is used to denote the position coordinate of the δ -potential impurity.

We calculate $A, B, C, D, E, F, G, H, J, K, L$ and M numerically from Eqn. 12, Eqn. 13 and Eqn. 14. Persistent current is defined by

$$I = \int_{-\frac{W}{2}}^{\frac{W}{2}} \frac{\hbar}{2im} (\Psi^\dagger \vec{\nabla} \Psi - \Psi \vec{\nabla} \Psi^\dagger) dy \quad (17)$$

which can be simplified to give

$$I = I^{(k_1)} + I^{(k_2)} \quad (18)$$

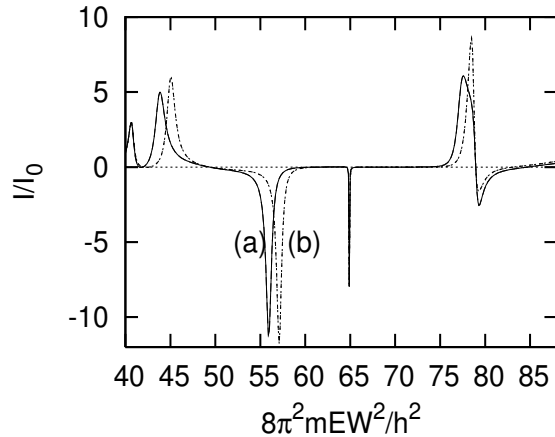


FIG. 3: I/I_0 vs $8\pi^2 mEW^2/\hbar^2$ with (a) $\gamma = 0$ (solid line) and (b) $\gamma = 4$ (dashed line). The system parameters are $l_1 = l_2 = l_3 = 1$, $\alpha = \beta = 0.3$.

Here

$$I^{(k_1)} = 2I_0(|E|^2 - |F|^2 + |G|^2 - |H|^2)^{(k_1)} \quad (19)$$

is the current when electron is incident along the left lead in k_1 channel. This is the scattering problem defined by Eqn. 12, Eqn. 13 and Eqn. 14. Similarly,

$$I^{(k_2)} = 2I_0(|E|^2 - |F|^2 + |G|^2 - |H|^2)^{(k_2)} \quad (20)$$

is the current when electron is incident along the left lead in k_2 channel and this scattering problem has to be solved by using a similar set of equations. Here, $I_0 = \frac{\hbar e}{2mW^2}$.

The nature of current obtained from Eqn. 18 is shown in Fig 3. We take the energy range ($4\pi^2 \leq \frac{2mEW^2}{\hbar^2} \leq 9\pi^2$, i.e. $40 \leq \frac{2mEW^2}{\hbar^2} \leq 88$) in such a way that both the modes are propagating. This gives the behavior that is captured in earlier works^{10,11,14}. The single ring current can be paramagnetic as well as diamagnetic as can be seen from Fig. 3. We shall show that when we make one of the modes evanescent, we will get a behavior that is not discussed before. As soon as $2mEW^2/\hbar^2$ becomes less than $4\pi^2$, the second channel becomes evanescent. This is because k_1 is real, whereas k_2 is imaginary ($k_2 \rightarrow i\kappa_2$ in this regime). No electron can be incident into an evanescent channel from infinity and so $I^{(k_2)}$ will not exist. But electrons incident in k_1 channel can be excited into an evanescent channel in the ring implying that G

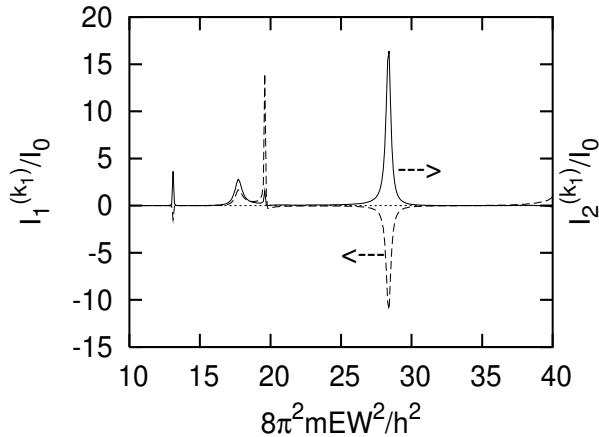


FIG. 4: $I_1^{(k_1)}/I_0$ and $I_2^{(k_1)}/I_0$ vs $8\pi^2 mEW^2/h^2$. The system parameters are $l_1 = l_2 = l_3 = 1$, $\alpha = \beta = 0.3$, $\gamma = 4$.

and H in Eqn. 19 are non-zero. A single impurity can excite an electron into the evanescent second channel. Scattering at the junctions can also excite an electron into the evanescent second channel. An electron residing in an evanescent state will carry a current. This naturally arises in the scattering problem that is defined in Eqns. 12-14. Evanescent mode current can be calculated by directly applying Eqn. 17 to evanescent mode wave-functions or it can be calculated by analytically continuing propagating mode current to below the barrier. Both results are equal.

The S matrix becomes 2×2 and is given by

$$S = \begin{pmatrix} r'_{11} & g'_{11} \\ g'_{11} & r'_{11} \end{pmatrix} \quad (21)$$

Although the S matrix is 2×2 , its calculation has to be done by using the 6×6 junction matrix S_J defined in Eqn. 10 and the 4×4 impurity S -matrix defined in Eqn. 14. g'_{12} , r'_{12} etc are still non-zero, although they do not carry any current but they define the coupling to the evanescent mode. So Eqns. 12, 13 and 14 still holds with $k_2 \rightarrow i\kappa_2$ where $\kappa_2 = \sqrt{\frac{4\pi^2}{W^2} - \frac{2mE}{\hbar^2}}$. Unitarity should imply $|r'_{11}|^2 + |g'_{11}|^2 = 1$ and indeed we get this from the junction matrix defined by S_J in Eqn. 10 and impurity S -matrix defined in Eqn.14. This implies that S_J is appropriate to account for realistic multichannel situations. S_U does not take into account such

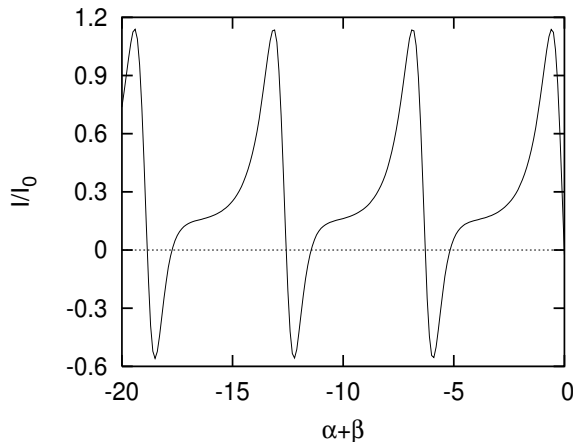


FIG. 5: I/I_0 vs $\alpha+\beta$ when second channel is evanescent. Here $l_1 = 1.0$, $l_2 = 0.2$, $l_3 = 1.8$ and $\gamma = -4.11$.

effects and does not allow one to include coupling to evanescent modes, maintaining unitarity. Current is expected to be continuous as the energy changes continuously from evanescent modes to propagating modes at $\frac{2mEW^2}{\hbar^2} = 4\pi^2$. This also comes out in our calculations

Note from Eqn. 19 that $I^{(k_1)} = I_1^{(k_1)} + I_2^{(k_1)}$, where $I_1^{(k_1)} = 2I_0(|E|^2 - |F|^2)^{(k_1)}$, E and F being the wave function amplitudes in the propagating channel and $I_2^{(k_1)} = 2I_0(|G|^2 - |H|^2)^{(k_1)}$, G and H being the wave-function amplitudes in the evanescent channel. In Fig. 4 we have plotted $I_1^{(k_1)}$ and $I_2^{(k_1)}$ versus $2mEW^2/\hbar^2$. While $I_1^{(k_1)}$ can be positive (diamagnetic) as well as negative (paramagnetic), $I_2^{(k_1)}$ is seen to be only diamagnetic. $I_2^{(k_1)}$ is the current in an evanescent channel, and there is a fundamental difference with evanescent channel currents in 1D. In 1D evanescent channel current cannot oscillate with energy because evanescent wave-function is not of wave nature²². In 1D we have to introduce an infinitesimal region of the ring where the electron can be propagating (evanescent in the rest of the ring), for the persistent current to be oscillating between paramagnetism and diamagnetism²³. But in the present case the second channel is evanescent throughout the length of the ring, its wave-function is not of wave nature, and yet can oscillate with Fermi energy. The peaks in $I_1^{(k_1)}$ are resonance effects due to wave nature of electron wave-function wherein at these energies, the electrons can spend a long time in the propagating mode. The impurity also gets a long time to pump

more electrons into the evanescent mode. So the evanescent mode current $I_2^{(k_1)}$ also peaks at the same energies where $I_1^{(k_1)}$ peaks (see Fig. 4) although the evanescent mode wave-function is not of wave nature. The difference between them being that while the peaks in $I_1^{(k_1)}$ can be in positive direction (diamagnetic) or in negative direction (paramagnetic), the peaks in $I_2^{(k_1)}$ are, always in the positive direction. As impurity configuration changes, these peaks also change randomly. But the peaks in $I_2^{(k_1)}$ always follow the peaks in $I_1^{(k_1)}$. One can also see this mathematically. Although the evanescent mode wave-function is not of a wave nature, G and H are functions of k_1 and κ_2 , due to the non-locality of quantum mechanics. E and F are also functions of k_1 and κ_2 . While $I_1^{(k_1)}$ will fluctuate around zero value, $I_2^{(k_1)}$ will fluctuate around a certain positive value as disorder configuration changes. Apart from this shift, $I_2^{(k_1)}$ will follow the same rules as $I_1^{(k_1)}$ as far as disorder averaging is concerned. Or more appropriately, $I_2^{(k_1)}$ will follow same averaging rules as conductance that fluctuate with disorder, remaining positive all the time. It is much easier to take random values of l_2 and l_3 to show this for the average current.

The observable current $I = I^{(k_1)}$ when second channel is evanescent, is plotted versus flux in Fig. 5. The figure shows that when a diamagnetic component is present, the response looks like that observed in experiments done by Deblock et al⁹. One can further check the validity of our explanation by measuring how the response of the ensemble scales with the number of rings in the ensemble. One has to go to a large enough ensemble so that the first harmonic has averaged to a flux independent diamagnetic component. This component will scale linearly with N , the number of rings present in the ensemble, while the flux dependent part will scale as \sqrt{N} .

Solution of Schrödinger equation in multichannel rings consist of evanescent modes that are naturally populated due to scattering. These evanescent modes can carry large persistent current that are diamagnetic in nature and are as sensitive to disorder as propagating modes. Previous attempts to explain the experimental results on persistent current ignore their contribution as they were thought to be small and insensitive to disorder. They provide a natural explanation for the discrepancy between theory and experiments. Future experiments should

try to isolate the role of the contributions coming from propagating and evanescent modes.

The authors would like to acknowledge useful discussions with Prof. A.M. Jayannavar. One of us (PSD) would like to acknowledge useful discussions with Prof. H. Bouchiat.

-
- ¹ M. Büttiker, Y. Imry and R. Landauer, Phys. Lett. **96A**, 365 (1983).
 - ² V. Chandrasekhar et al, Phys. Rev. Lett. **67**, 3578 (1991).
 - ³ D. Maily, C. Chapelier and A. Benoit, Phys. Rev. Lett. **70**, 2020 (1993).
 - ⁴ E. M. Q. Jariwala, P. Mohanty, M. B. Ketchen and R. A. Webb, Phys. Rev. Lett. **86**, 1594 (2001).
 - ⁵ W. Rabaud et al, Phys. Rev. Lett. **86**, 3124 (2001).
 - ⁶ L. P. Levy, G. Dolan, J. Dunsmuir and H. Bouchiat, Phys. Rev. Lett. **64**, 2074 (1990); L. P. Levy, Physica (Amsterdam) **169B**, 245 (1991).
 - ⁷ B. Reulet, M. Ramin, H. Bouchiat and D. Maily, Phys. Rev. Lett. **75**, 124 (1995).
 - ⁸ R. Deblock, Y. Noat, H. Bouchiat, B. Reulet and D. Maily, Phys. Rev. B **65**, 075301 (2002).
 - ⁹ R. Deblock, R. Bel, B. Reulet, H. Bouchiat and D. Maily, Phys. Rev. Lett. **89**, 206803 (2002).
 - ¹⁰ G. Montamboux, H. Bouchiat, D. Sigeti and R. Friesner, Phys. Rev. B **42**, 7647 (1990).
 - ¹¹ V. Ambegaokar and U. Eckern, Phys. Rev. Lett. **65**, 381 (1990).
 - ¹² B. L. Altshuler, A. G. Aronov and B. Z. Spivak, JETP Lett. **33**, 94 (1981).
 - ¹³ D. Y. Sharvin and Y. V. Sharvin, JETP Lett. **34**, 272 (1981).
 - ¹⁴ A. Schmid, Phys. Rev. Lett. **66**, 80 (1991).
 - ¹⁵ P. Koskinen and M. Manninen, Phys. Rev. B **68**, 195304 (2003).
 - ¹⁶ V. E. Kravtsov and B. L. Altshuler, Phys. Rev. Lett. **84**, 3394 (2000).
 - ¹⁷ M. Pascand and G. Montamboux, Europhys. Lett. **37**, 347 (1997); Phys. Rev. Lett. **82**, 4512 (1999).
 - ¹⁸ P. S. Deo and A. M. Jayannavar, Mod. Phys. Lett. B **7**, 1045 (1993).
 - ¹⁹ M. Büttiker, Phys. Rev. B **32**, 1846 (1985).
 - ²⁰ M. Büttiker, Y. Imry and M. Ya. Azbel, Phys. Rev. A **30**, 1982 (1983).
 - ²¹ Philip F. Bagwell, Phys. Rev. B **41**, 10354 (1990).
 - ²² P. Singha Deo, Phys. Rev. B **53**, 15447 (1996).
 - ²³ C. Benjamin and A. M. Jayannavar, Phys. Rev. B **68**, 085325 (2003).